PHILOSOPHICAL TRANSACTIONS OF THE ROYAL SOCIETY A MATHEMATICAL, PHYSICAL & ENGINEERING SCIENCES

Hydrodynamics and Sediment Dynamics of North Sea Sand Waves and Sand Banks [and Discussion]

D. A. Huntley, J. M. Huthnance, M. B. Collins, C.-L. Liu, R. J. Nicholls, C. Hewitson, M. O. Green, K. R. Dyer and C. F. Jago

Phil. Trans. R. Soc. Lond. A 1993 **343**, 461-474
doi: 10.1098/rsta.1993.0059

Hydrodynamics and sediment dynamics of North Sea sand waves and sand banks

By D. A. Huntley[1], J. M. Huthnance[2], M. B. Collins[3], C.-L. Liu[1], R. J. Nicholls[1] and C. Hewitson[3]

[1] *Institute of Marine Studies, University of Plymouth, Drake Circus, Plymouth, Devon PL4 8AA, U.K.*

[2] *Proudman Oceanographic Laboratory, Bidston Observatory, Birkenhead L43 7RA, U.K.*

[3] *Department of Oceanography, The University, Southampton SO9 5NH, U.K.*

Seabed drag coefficients have been measured at a site within the Norfolk Banks and at a site within the sand wave field in the southern North Sea, using pressure sensors and moored current meters. At the sand banks site a seabed tripod measuring turbulent flows within 1 m of the bed was also used. The results are generally in agreement with values used in numerical models. At the sand banks site, the drag coefficient increases with wind conditions, but at the sand waves site there is a *reduction* during the highest wave conditions, attributed to the drag reduction caused by sand resuspension from the bed. This result suggests that sediment effects must be considered if wave/current interaction is included in numerical models of the region. The drag coefficient for reversing tidal flows over the asymmetric sand waves is found to be larger for flow towards the steeper face, suggesting a small form drag component.

Studies of sand movement used bedform mapping, fluorescent sand tracing and photography of migrating ripples. There is evidence for the early stages of formation of a new bank between Broken Bank and Well Bank. At the sand waves site, ripple migration is found to be a useful estimator of bedload transport under conditions of negligible suspension.

Over the sand banks, a definite correlation of surface water properties, notably the turbidity, with the topography of the banks was observed. The mechanism for this surface effect is not known but it is consistent with the observation of features, seen in satellite visible light images, which outline the shapes of the banks.

1. Introduction

Bedforms on a variety of spatial scales occur widely over the sandy seabed of the southern North Sea. The sand wave field covers an area of at least 15000 km^2 (figure 1) and sand banks occur in several areas, most notably off the Norfolk coast of the U.K.

Interest in these features within the context of the North Sea Programme centres on their potential importance for numerical modelling of the hydrodynamics of the region, and on the mobility of the sand and hence the stability of the features and the potential for sediment resuspension. This paper describes both hydrodynamic and sediment dynamic measurements at two sites in the southern North Sea, one

Phil. Trans. R. Soc. Lond. A (1993) **343**, 461–474
Printed in Great Britain

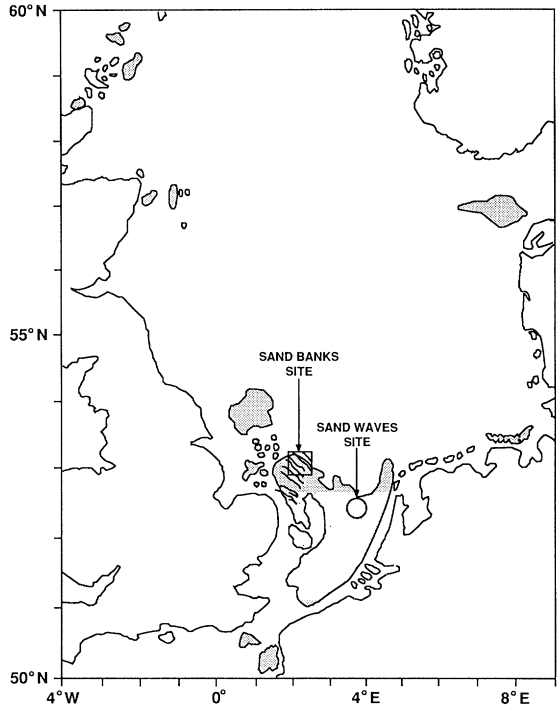

Figure 1. Location map. The shaded region shows the extent of sand waves in the North Sea.

within a field of relatively uniform sand waves and the other near Broken Bank within the Norfolk Banks (figure 1).

2. The field sites

(*a*) *Sand waves site*

Selection of a field site within the sand wave field in the southern North Sea was determined by the need for a swath, about 10 km long, of relatively regular sand waves, in both height and wavelength, with the 10 km distance dictated by the need for good resolution of the pressure gradients using spatially separated pressure sensors (Huntley *et al.* 1993). The site chosen was centred at 52° 10′ N; 3° 46′ E, where sand waves are typically 3 m high with wavelengths of 200 m. Figure 1 shows the location chosen, and figure 2 shows part of an echo-sounding transect along the 10 km swath. The asymmetry of the sand wave profiles in this region is evident in figure 2, and the steeper north-facing slope suggests sand transport towards the north. The mean sand grain diameter over the sand waves was 0.29 mm.

(*b*) *Sand banks site*

The Norfolk Banks are located approximately 100 km offshore of the East Anglian coastline (figure 1). The Banks are up to 55 km long, 5 km wide and rise up to 35 m above the surrounding seabed. Some reach to within 5 m of the sea surface. The study area was within the Well, Broken and Swarte Banks system (figure 3). These Banks are asymmetric in cross section, with steep north-eastern lee slopes and more gently sloping south-western stoss slopes. The grain size of surficial sediments around the Broken Bank is predominantly fine sand, with a mean grain size of 0.2 mm.

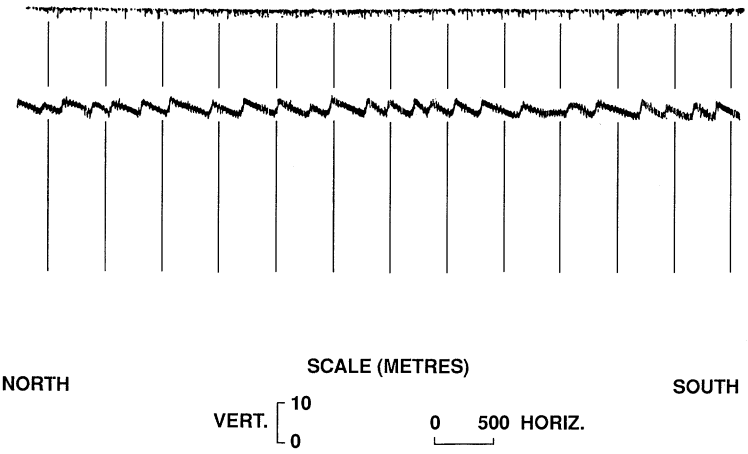

Figure 2. A section of an echo-sounder transect between the pressure sensors at the sand waves site.

3. Frictional drag at the seabed

(*a*) *Principles*

The frictional drag at the seabed is estimated from simultaneous measurement of pressure gradients and of the currents driven by those pressure gradients. At both the sand waves and the sand banks sites the pressure gradient could only be determined in one horizontal direction, *along* the sand bank axis at the sand banks site and *perpendicular* to the sand waves crests at the sand waves site.

The seabed drag, τ_b, is assumed to take the form of a quadratic stress:

$$\tau_b = \rho C_d\, u(u^2+v^2)^{\frac{1}{2}},$$

where (u, v) is the horizontal current vector at a reference height above the bed, C_d is a dimensionless drag coefficient and ρ is the density of seawater, taken as 1027 kg m^{-3}. At both sites the currents were measured at approximately mid-water depth and are therefore within a few percent of the depth-averaged currents (for example at the sand waves site the difference between measured and depth-averaged current is estimated to be less than 5%). This difference is much smaller than the scatter in drag coefficient values (e.g. table 2) and we therefore assume that the drag coefficients are appropriate to depth-averaged current speeds.

The equation for the depth-averaged momentum balance in the direction of the u current takes the form:

$$\rho\frac{\partial u}{\partial t}+\rho u\nabla u-\rho fv=-\frac{\partial p}{\partial x}-\frac{\tau_b-\tau_w}{h},$$

where p is the pressure at the sea bed, h is the water depth, f is the (latitude dependent) Coriolis parameter, τ_w is the u-component of the wind stress acting on the water surface and τ_b is the bed stress. This equation can be rearranged into the following form:

$$\underbrace{\rho\frac{\partial u}{\partial t}+\rho u\nabla u}_{\text{ACC}}-\ \rho fv\ +\ \frac{\partial p}{\partial x}\ -\ \frac{\tau_w}{h}\ =-C_d\rho\frac{(u^2+v^2)^{\frac{1}{2}}u}{h},$$

$$\text{SUM} \equiv \text{ACC} - \text{CORIO} + \text{PGRAD} - \text{WNDSTR} = -C_d\ \text{BTMSTR}.$$

The terms BTMSTR, ACC and CORIO can be evaluated from moored current meter

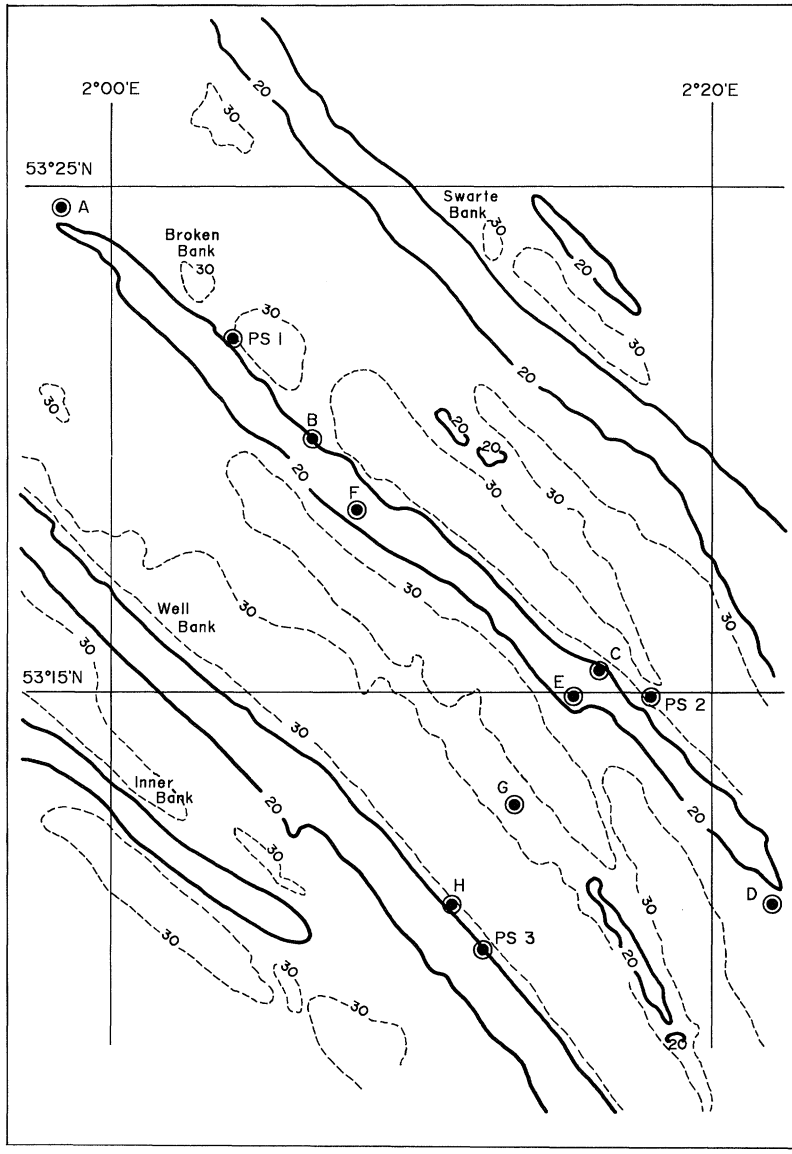

Figure 3. Map of the sand banks site. Data discussed in the paper come from the pressure sensors at PS1 and PS2, and current meters at B and F.

measurements. At both sites the advective component of ACC was found to be relatively small (at most a few percent of the linear terms) and was neglected. The time derivative was evaluated as a difference of adjacent 15 min values.

The wind stress term, WNDSTR, was assumed to be quadratic in the wind speed:

$$\tau_w = \rho_a C_w w^u |w|,$$

where ρ_a is the density of air (taken to be 1.25 kg m^{-3}), w is the magnitude of the wind speed at a height of 10 m, w^u is the wind speed component in the direction of the current u, and C_w is a drag coefficient appropriate to the 10 m wind height. For the sand banks site, winds were interpolated in space and time from three-hourly values,

Table 1. *Data for the sand banks site*

mooring	position		depths/m		time, day (1988)		sampling
	latitude (°N)	longitude (°E)	water	instr.	begin	end	min
PS1	53 22.09	02 04.07	33	33	19.625, 322	10.875, 407	15
PS2	53 14.85	02 17.89	35	35	08.625, 322	14.875, 351	15
B	53 19.9	02 06.5	26	16	15.6, 322	07.4, 332	2
F	53 18.6	02 08.1	19	9	09.1, 321	08.8, 332	2

provided by the UK Meteorological Office from the Numerical Weather Prediction model during its data assimilation runs. Sand banks C_w values were based upon Smith & Banke (1975), taking the form:

$$C_w = (0.63 + 0.066\, w) \times 10^{-3}.$$

For the sand waves site, hourly wind speeds and directions at 10 m height recorded at the Leman gas rig, about 70 km to the west of the site, were used. Possible consequences of the 70 km separation are discussed by Huntley *et al.* (1993), but are generally not expected to be significant. For these data a slightly different form of wind drag coefficient was used, suggested by Gill (1982) and based upon Smith (1980):

$$\begin{aligned} C_w &= 1.1 \times 10^{-3} && \text{for } w < 6 \text{ m s}^{-1} \\ &= (0.61 + 0.063w) \times 10^{-3} && \text{for } 6 < w < 22 \text{ m s}^{-1}. \end{aligned}$$

The pressure gradient term PGRAD was measured at each site from pairs of separated pressure sensors, but includes an unknown constant due to the unknown relative vertical levels of the sensors. This unknown constant term can be eliminated by considering only the time-varying component of each of the terms; Huntley *et al.* (1993) consider the semi-diurnal tidal constituent. Alternatively the drag coefficient can be evaluated as the slope of the regression of SUM against BTMSTR; the intercept of the regression line at zero BTMSTR gives the unknown constant. In the present work we use the latter technique.

(*b*) *Data*

Pressure and current sensors were deployed at the sand waves site in October/November 1988. The two pressure sensors were located 11.2 km apart along a line perpendicular to the local sand wave crests (N27° E), and were deployed in sand wave troughs, where variations in pressure due to uncertainty in sensor location were minimized. The current meter, an S4, was moored 8 km east of the line joining the pressure sensors, at 12 m above the bed in a depth of 29 m.

Figure 3 shows the locations of the sensors deployed at the sand banks site, for a period of about 11 days in November 1988. Restricting attention to good data has limited the analysis here to pressure sensors PS1 and PS2, and the mid-water current records at B and F, 'between' them. Table 1 summarizes the data used in this study.

(*c*) *Results from the sand banks site*

The drag coefficient, C_d was estimated by regressing SUM against BTMSTR for the whole period (days 322–332) and also for each individual day to give a time series for comparison with possible controlling factors. However, it was noticed that the daily

Table 2. *Drag coefficient results for sand banks site*

(±s.d. values assume independent ½-hourly data; correction may entail a factor of 2.)

	$10^3 \times C_{\|}$(±s.d.)		corrl. coeff. (r^2)		SUM leads/h	
day	B	F	B	F	B	F
322–332	3.23±0.24	0.46±0.17	0.29	0.02	n.a.	n.a.
323	6.32±0.60	4.64±0.69	0.71	0.50	−0.1	0.5
324	5.81±0.56	2.03±0.36	0.70	0.41	−0.6	−0.5
325	5.84±0.37	2.33±0.42	0.85	0.40	−0.6	−0.3
326	4.41±0.49	1.42±0.38	0.64	0.23	−0.4	−0.0
327	4.15±0.55	2.93±0.28	0.55	0.71	2.2	3.1
328	3.96±0.60	3.01±0.22	0.48	0.80	2.9	3.2
329	3.80±0.52	2.82±0.19	0.54	0.84	2.9	3.3
330	3.76±0.51	2.76±0.22	0.54	0.78	2.6	3.3
331	3.62±0.52	3.16±0.23	0.51	0.80	2.8	3.4

C_d values decreased sharply on day 327, owing to the development of a phase difference, with SUM leading BTMSTR. Accordingly, table 2 shows daily estimates of C_d based on the *phase-lagged* regression giving the maximum correlation coefficient. The time lags applied are also shown in table 2.

The change of phase between SUM and BTMSTR is quite abrupt. It occurs during the transition from neap to spring tides, but perhaps more significantly at the time of a sharp increase in wind stress, accompanied by an increase in the amplitude of PGRAD.

A problem with the timing of one of the two pressure records might be suspected; however, their residuals after tidal analysis match to within a few mb and do not show any distinct tidal signal to either side of day 326/7 that would correspond to the observed phase change. The currents are not suspect because the phase change is common to B and F. The reasons for the phase shift therefore remain unresolved.

The bottom mounted tripod STABLE (Humphery 1987) was also deployed at the Sand Banks site (at 53° 14.6′ N; 2° 14.5′ E) and collected current and turbulence data from electromagnetic current meters at two levels within 1 m of the bed spanning days 324–326. Bottom stress has been estimated as the Reynolds stress, τ_r, the time average of the product of vertical and along-flow turbulent currents. Regression shows that a bottom stress relation,

$$\tau_r/\rho = C_r|U_{100}|^2,$$

is a good representation of the data ($r^2 = 0.826$) without significant delay between τ_r and $|U_{100}|^2$, where U_{100} is the velocity 1 m above the bottom. The value of C_r is estimated as 3.2×10^{-3}. The associated value of bottom roughness z_0 is $\exp(-\kappa/C_r^{\frac{1}{2}})$, and gives 0.9 mm, corresponding to coarse sand or the presence of slight bedforms.

These results are discussed in relation to the sand waves results in §3*f*.

(*d*) *Results from the sand waves site*

Daily variations in the drag coefficient at the sand waves site were calculated by regressions between SUM and BTMSTR for 24 h data segments, with a 12 h overlap between adjacent segments. The resulting time series of drag coefficient over the 27-day period is shown in figure 4. This figure also shows the time series of drag coefficient calculated for the total semidiurnal (Z_2, based on only 24 h of data) tidal component by Huntley *et al.* (1993). As expected for this site, where semi-diurnal

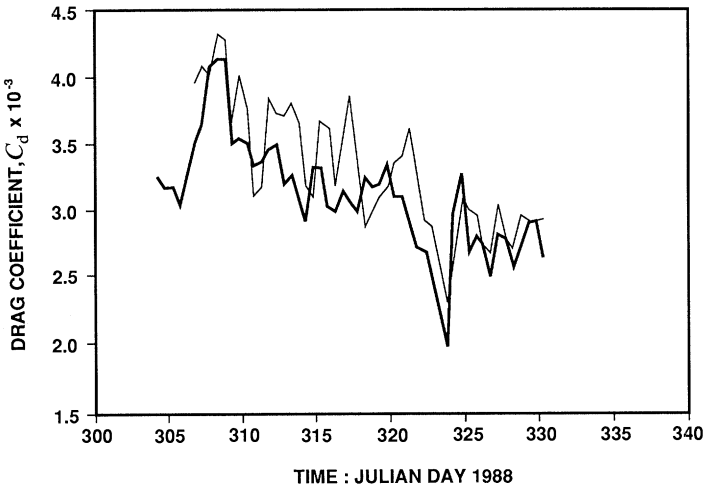

Figure 4. Time series of drag coefficient at the sand waves site. The light line shows values computed by the regression method, and the heavy line shows those for the Z_2 component only.

currents dominate, the agreement between the two estimates of drag coefficient is good both in shape and magnitude, through the Z_2 estimate tends to be somewhat smaller.

In view of the strong asymmetry of the sand waves at this site (figure 2) separate regressions have been calculated for positive currents (to the north) and negative currents (to the south). For the complete data-set, these regressions give drag coefficients to the north and south, C_{dN} and C_{dS}, respectively, of

$$C_{\mathrm{dN}} = (2.5 \pm 0.2) \times 10^{-3},\ C_{\mathrm{dS}} = (3.0 \pm 0.3) \times 10^{-3},$$

where the error bound is the standard deviation of the regression.

As might be expected, these results suggest that the drag coefficient is larger for flow facing the larger slope of the asymmetric sand waves, though the difference is bridged by the standard deviations of each fit and is therefore not well established. Section 3*f* discusses this result in relation to a model for flow over bedforms.

One surprising result is that the regression intercept varies systematically over the 27-day period. Figure 5 shows this variation for both the northwards and southwards flows. Also shown in figure 5 is the 24 h averaged pressure difference between the pressure sensors; the correlation with intercept variation is strong.

Reasons for this variation in intercept are unclear. The intercept is expected to represent the mean pressure gradient resulting from deployment of the two pressure sensors at different geopotential levels. The observed variation covers a range of about 4 mb which is large compared to any expected vertical movement of the pressure mounts, particularly as it continues throughout the 27-day period. Correlation of the pressure difference with measured 24 h averaged flow is poor, and the flows are in any case only $O(0.05\ \mathrm{m\ s^{-1}})$, an order of magnitude smaller than would be driven by the observed variation in pressure difference. As already indicated, the omitted nonlinear terms in the momentum equation are too small to explain the variation; in addition, they would influence only the slope, not the intercept, of the regressions. The most likely cause of the variation must therefore be long-term drift in one or both of the pressure sensors, though a drift of this magnitude is unexpected.

PHILOSOPHICAL TRANSACTIONS OF THE ROYAL SOCIETY A MATHEMATICAL, PHYSICAL & ENGINEERING SCIENCES

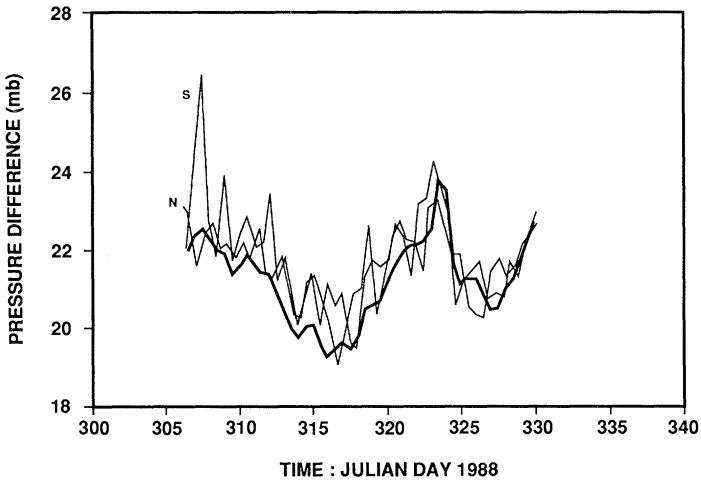

Figure 5. Time series of the intercepts of the regression fits for northerly and southerly flows (light lines), and the 24 h averaged pressure difference (heavy line), for the sand waves site.

(*e*) *Error analysis*

Excepting $\partial p/\partial x$, the magnitude of the terms in the momentum balance are individually accurate to $O(\Delta u/u)$, where Δu is a velocity measurement error; for the present data sets this error is expected to be relatively small (a few percent). The pressure gradient term is of similar accuracy ($O(5\,\%)$) for the recorded pressure differences but is particularly sensitive to any unidentified error. The SUM term of course has the cumulative errors from the contributing terms so might be expected to be known to within $O(20\,\%)$. However, Huntley *et al.* (1993) conclude that errors in SUM (and hence in C_d) are particularly sensitive to errors in the *phase* of the current measurements, a 1° error causing a change of almost 5% in drag coefficient. Uncertainties in the phase of the currents arise from both the horizontal separation of the current meter from the pressure sensor line and possible changes of phase with depth through the water column, the latter being of particular significance in the relationship between measured and depth-averaged currents. These phase uncertainties can contribute to a systematic error in C_d and possibly also, through time dependence, to reduced linear correlation between SUM and BTMSTR.

At the sand banks site such phase differences probably account for the different values of C_d obtained from B (larger) and F. At the sand waves site numerical models suggest that the phase differences over the 8 km separation of the current meter from the pressure sensor line are only $O(0.7°)$ and vertical differences in phase are likely to be small at this shallow (29 m) site. Overall, potential systematic errors in C_d at the sand waves site are estimated to amount to about 10%.

(*f*) *Discussion*

The values of drag coefficient found for both the sand banks and sand waves sites are generally similar. At the sand waves site the overall Z_2 value for the 27-day period was found to be 2.95×10^{-3}. At the sand banks site the average of the phase-adjusted daily values using the currents at F is 2.79×10^{-3}. There is also reasonable agreement between the STABLE estimate of drag coefficient between days 324 and 326 and the estimates for the same period from F. The drag coefficient from STABLE relates to currents at 1 m off the bed while the drag coefficients in table 2 relate to

PHILOSOPHICAL TRANSACTIONS OF THE ROYAL SOCIETY A MATHEMATICAL, PHYSICAL & ENGINEERING SCIENCES

mid-water depth currents. However, if these drag coefficients are converted to equivalent bottom roughnesses (assuming a logarithmic layer extending at least to mid-water) values of 0.9 mm for STABLE and 1.0 mm for the average F drag coefficient are obtained between days 324 and 326; given the high sensitivity of the bottom roughness to small errors in C_d, this agreement is encouraging. The agreement between estimates based on currents 1 m above the bed and at mid-depth also implies that form drag due to larger scale bedforms (megaripples or sand waves) was negligible at this site.

The much larger values of drag coefficient from currents at B are apparently at variance with the other estimates. These values may reflect larger bed roughness or bedforms at site B, located on the steeper northeast-facing slope of the Bank, though the roughness length associated with the average of the daily values in table 2 is 42 mm, a larger than expected value even for a region of large bedforms.

There is some evidence that the response of the drag coefficient to high waves and wind differs at the two sites. At the sand waves site, the largest wave event, on day 323, is associated with a *reduction* in drag coefficient (figure 4). Huntley *et al.* (1993) hypothesize that this reduction is due to suspension of sand during high waves which causes stable stratification of the water column near the bed which in turn causes a drag reduction at the bed, as suggested by Glenn & Grant (1987). At the sand banks site, in contrast, the *largest* values of C_d occur on day 323. This may be because there is a minimal fine-sediment fraction available for suspension in the generally higher energy current régime over the banks, so that the stress enhancement due to wave/current interaction dominates. It is also worth noting that the change in the current-stress phase between days 326 and 327 also coincides with the development of the next largest wind stress event in the record.

The results for northwards and southwards flows at the sand waves site suggest that the asymmetric shape of the sand waves results in a different drag coefficient for flood and ebb tidal flows. Qualitatively these results agree with numerical model predictions made by Richards (1982) for bedforms of similar asymmetry but the predicted differences are an order of magnitude smaller than those observed. This disagreement is probably because the published model runs use a bed roughness which is an order of magnitude smaller than that found at the sand waves site. The model is currently being run with realistic bed roughness to simulate more accurately the field conditions.

The varying phase relationship between apparent stress and current and the need to include sediment suspension effects suggests that detailed modelling of the time-dependent nearbed flow is necessary. Numerical models of this complexity capable of resolving sand bank bathymetry need a fine grid (O(100 m)) and present a large computational requirement, but are now becoming feasible. Such a calculation is in prospect (A. M. Davies, personal communication) for the area of Broken Bank.

4. Sediment movement

(*a*) *Measurements*

A number of different techniques were used to investigate sediment movement. The Southampton group, working at the sand banks site, used: continuous monitoring of surface water turbidity, for suspended sediment determination; deployment of a CTD system, with transmissometer attached, to determine tidal-cycle variability in the structure of turbidity and its relationship to characteristics

PHILOSOPHICAL TRANSACTIONS OF THE ROYAL SOCIETY A MATHEMATICAL, PHYSICAL & ENGINEERING SCIENCES

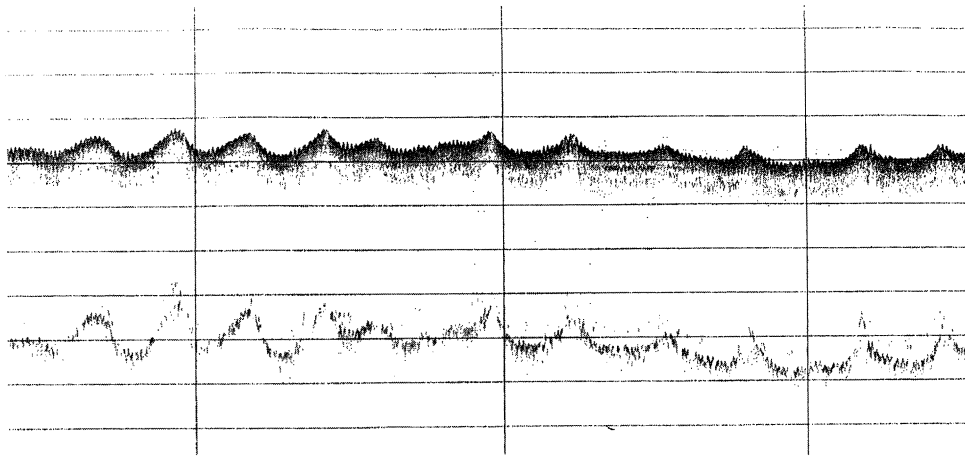

Figure 6. Part of an echo-sounding at the sand banks site, near 53° 20′ N; 2° 00′ E. The horizontal length of the transect is 8704 m, and the vertical spacing of the grid lines is 7.5 m. The asymmetric shapes of the sand waves suggests convergence of sand transport towards the centre of the transect.

of the water masses; side-scan sonar, to identify bedforms (megaripples and sand waves); the release of coloured fluorescent sand at two locations, with subsequent sampling; and the deployment of the STABLE tripod, equipped with OBS (optical back scatter) sensors for suspended sediment and a camera system for observing bedform migration. At the sand waves site a deployment of STABLE for the Plymouth group provided photographs of migrating bedforms, from which estimates of bedload transport were computed.

(*b*) *Results*

Sand wave asymmetry at the sand banks site indicates sand movement onto the banks from either side. A feature of particular interest is the observed reversal of sand wave asymmetry at a location in the swale between Broken Bank and Well Bank (near 53° 20′ N; 2° 00′ E), shown in the echo-sounding (figure 6). This reversal of asymmetry implies (Langhorne 1982) convergence of sand transport towards a location *between* the main sand banks, and may thus represent the initial stages of the formation of a new sand bank.

Also at the sand banks site a strong correlation between surface water properties and the water depth was measured. The correlation with surface turbidity is illustrated in figure 7, which shows the variation in water surface properties for a transect towards the north-northeast from 53° 02′ N; 2° 14′ E, crossing Well Bank just after 1800 h and Broken Bank just before 1930 h. At about 1940 h the ship reversed direction and recrossed Broken Bank at 2000 h. High suspended particulate matter (SPM) concentrations are located over the crests of the banks. This correlation of bathymetry with SPM levels was found to be more consistent than with either temperature or salinity, though some transects showed strong temperature variations, of the order of 0.2 °C.

This observation of a surface signature of the topography of the banks is important for the interpretation of remote-sensed images of the region. Some satellite images clearly show the presence of the banks and delineate their form accurately. An example can be found in the CZCS Band 3 image of the southern North Sea in Holligan

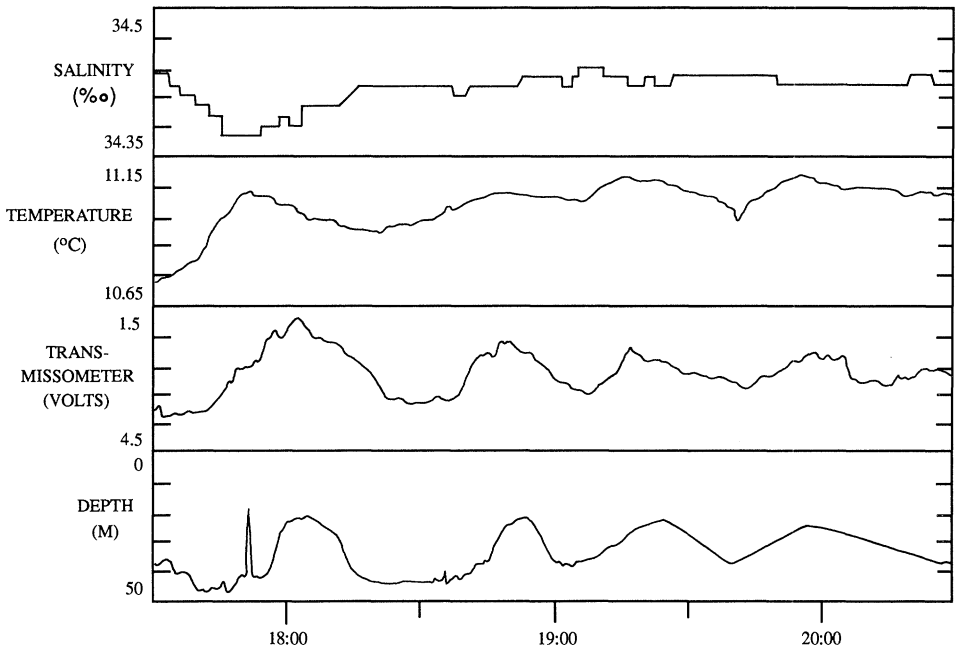

Figure 7. Time series of surface water properties and water depth in the sand banks region. The correlation between depth and surface transmission is striking.

et al. (1989; fig. 15, see also fig. 29). Various explanations have been suggested for this optical remote imaging of features related to subsurface topography. Hennings *et al.* (1988) considered the influence of suspended sediments, reflection from the sea floor, and variations in sea surface roughness associated with wind and tidal flows, and they concluded that specularly reflected sunlight at the rough ocean surface was the dominant mechanism. In contrast, the present observations show that surface water properties, notably the SPM levels, can be sufficient to produce the observed images.

At the sand waves site, a deployment of STABLE in February 1989 provided a sequence of seafloor photographs showing migration of ripples in response to the tidal flows. Huntley *et al.* (1991) assess the potential of these photographs for estimating bedload transport. They conclude that the sand transport implied by the migrating ripples is a good estimate of bedload transport under conditions where sand suspension is minimal, as at the sand wave site under normal conditions. They use the results in a test of a range of bedload transport formulae. It is clear from these observations that sand transport occurs over the sand waves even under normal tidal conditions, though the net transport has not been estimated, and storm conditions were not encountered during the measurement period.

5. Conclusions

The values of seabed drag coefficient obtained at both sites are generally in accord with those used in two-dimensional (vertically averaged) numerical models of the region. These results support the validity of the regression technique, though the regression coefficients shown in table 2 are relatively low, suggesting that $O(40\,\%)$

of the overall variance is unexplained. The discussion of potential errors in §3*e* leads to the conclusion that uncertainty in the phase of the currents is perhaps the most significant potential error in closing the dynamical balance. Whatever the cause, modelling or measurement of the full vertical structure of the tidal waves should help shed light on the remaining errors.

The drag coefficient values are larger than for a flat seabed, but there is little evidence for a large form drag contribution from the large-scale bedforms. At the sand banks site the agreement between the measured stresses based on the mid-water current meter at F and based on STABLE measurements 1 m above the bed suggests negligible form drag. The larger values based on mooring B could suggest a significant form drag contribution at that location, but the values appear to be anomalously high and may be in error. At the sand waves site there is some evidence for a form drag effect in the difference in drag coefficient for northward and southward flows across the asymmetric sand wave profiles. The magnitude of this difference is larger than predicted by modelling, but further model runs are needed with more realistic small-scale bed roughness. Overall the lack of a larger form drag component is consistent with the generally smooth relief of the large-scale bedforms.

The importance of including wave/current interaction in numerical models of the region appears to depend critically on the potential for sediment resuspension from the bed. At the sand banks site the drag coefficient is enhanced during the highest wind events, while at the sand waves site the drag coefficient is relatively insensitive to wind and wave conditions, even showing a decrease at the time of the largest wave event. This different behaviour is attributed to the influence of sediment resuspension at the sand waves site, which effectively causes drag reduction countering the wave/current enhancement. These results suggest that inclusion of wave/current effects in numerical models must be approached with caution, and that sediment effects should be included if appreciable resuspension is expected to occur.

The sediment results show appreciable sand movement at both sites, with some evidence for the formation of a new bank between Well Bank and Broken Bank.

The observation of a surface signature of the bank topography clearly has implications for the interpretation of optical satellite images, though the causes of these surface variations require further investigation.

References

Gill, A. E. 1982 *Atmosphere–ocean dynamics*. (662 pp.) New York: Academic Press.

Glenn, S. M. & Grant, W. D. 1987 A suspended sediment stratification correction for combined wave and current flows. *J. geophys. Res.* C**92**, 8244–8264.

Hennings, I., Doerffer, R. & Alpers, W. 1988 Comparison of submarine relief features on a radar satellite image and on a Skylab satellite photograph. *Int. J. Rem. Sensing* **9**, 45–67.

Holligan, P. M., Aarup, T. & Groom, S. B. 1989 The North Sea satellite atlas (ed. J. Aiken), *Continental Shelf Res.* **9**, 667–765.

Humphery, J. D. 1987 STABLE – an instrument for studying current structure and sediment transport in the benthic boundary-layer. In *Fifth International Conference on Electronics of Ocean Technology, Heriot-Watt University, Edinburgh*, pp. 57–62, London: Institution of Electronic and Radio Engineers. (225 pp.)

Huntley, D. A., Amos, C. L., Williams, J. J. & Humphery, J. D. 1991 *Estimating bedload transport on continental shelves by observations of ripple migration – an assessment. In Proc. Euromech 262: Colloquium on Sand Transport in Rivers, Estuaries and the Sea* (ed. R. Soulsby & R. Bettess), pp. 17–24. Rotterdam: Balkema Press.

Huntley, D. A., Nicholls, R. J., Liu, C.-L. & Dyer, K. R. 1993 Measurements of the semi-diurnal drag coefficient over sand waves. *Continental Shelf Res.* (In the press.)

Langhorne, D. N. 1982 A study of the dynamics of a marine sand wave. *Sedimentology* **29**, 571–594.

Richards, K. J. 1982 Turbulent flow over ripples and their effective roughness. In *Proc. Euromech 156: Mechanics of Sediment Transport* (ed. B. M. Sumer & A. Müller), pp. 127–131.

Smith, S. D. 1980 Wind stress and heat flux over the ocean in gale force winds. *J. Phys. Oceanog.* **10**, 709–726.

Smith, S. D. & Banke, E. G. 1975 Variation of the sea surface drag coefficient with wind speed. *Q. Jl R. met. Soc.* **101**, 665–673.

Discussion

M. O. Green (*Bullard Laboratories, University of Cambridge, U.K.*). Professor Huntley explained the curiously low drag coefficient observed during the period of relatively high wave activity as due to stable stratification of the boundary layer by the suspended-sediment load. But presumably a thick bedload layer would have formed at the same time, which is expected to extract momentum from the mean flow thereby enhancing the drag. Can these two processes with opposite effects on the mean flow be reconciled?

D. A. Huntley. Yes, to some extent we have been able to show that, though bedload transport would enhance the drag, the suspension effect is likely to dominate and cause an overall reduction in drag during the high wave event. In the paper describing the estimation of drag coefficients for the semidiurnal tidal components only (Huntley *et al.* 1993) I have used the numerical model of Glenn & Grant (1987) to simulate conditions at the sand waves site. This model includes wave/current interaction, bedform formation and both bedload and suspended sediment effects. For the high wave event a reduction in drag is predicted. The magnitude of the reduction is smaller than observed if mean grain diameter at the bed is used in the prediction, but prediction and observation can be reconciled if it assumed that a finer fraction of the grain size distribution at the bed is primarily involved in resuspension.

The data-set is too limited as yet to provide an unequivocal result, but there are strong indications that the suspension effect can effectively at least 'switch off', if not reverse, the expected wave/current (and bedload) enhancement.

K. R. Dyer (*University of Plymouth, U.K.*). In the analysis to obtain the drag coefficient, the constant term relates to the relative depths of the pressure sensors below 'mean sea level'. Professor Huntley has shown that this varies during the time series. Since the site is very close to the amphidromic point, could the change be related to the spring-neap variation in position of the amphidromic point? This might cause a time varying mean sea surface slope.

D. A. Huntley. Our measurements are certainly close to the amphidromic points of many of the tidal constituents; in fact the cross-spectra between the pressure sensor records suggest that the two sensors *span* the M8 amphidromic point. It must also be true that the location of the amphidromic points will have moved during the measurement period, as part of the spring-neap cycle and perhaps in response to surges, etc.

However, there does not seem to be any way in which this can explain our observation of a drift in the apparent relative depths of the pressure sensors. There

PHILOSOPHICAL TRANSACTIONS OF THE ROYAL SOCIETY A MATHEMATICAL, PHYSICAL & ENGINEERING SCIENCES

are two problems. Firstly the slope associated with an amphidromic point is, of course, not a mean sea surface slope but one which varies sinusoidally at the frequency associated with the point. Secondly, the dynamical balance of the depth-averaged momentum equation implies that any true sea surface slope will be associated with a flow; the apparent slopes shown in figure 5 are intercepts of the regression at zero flow.

C. F. Jago (*School of Ocean Sciences, University of Wales, U.K.*). Our observations at your sand wave site suggest that intermittent benthic anoxia may develop during the early summer plankton bloom. This implies that the bed must be stable for periods of a few days at least. Do the measurements show that there may be periods of little or no bed load transport during the spring/neap cycle?

D. A. Huntley. Unfortunately our observations of sediment movement at the seabed using photography from STABLE, described fully in Huntley *et al.* (1991), are of very limited duration, lasting approximately 72 h in February 1989. Nevertheless wave conditions were relatively low during this period (ratio of wave to tidal currents at the bed of approximately 0.2), and it was possible to estimate an approximate threshold for sand movement based on observation of ripple migrations. The mean flow threshold was estimated to be about 0.4 m s^{-1}.

The S4 measurements of tidal flow over the 27-day period show the maximum tidal flow falling below 0.4 m s^{-1} for six consecutive tidal cycles during the lowest neap conditions. Thus it appears that a combination of low waves and low neap tides could leave the bed undisturbed for a few days.

PHILOSOPHICAL TRANSACTIONS OF THE ROYAL SOCIETY A MATHEMATICAL, PHYSICAL & ENGINEERING SCIENCES

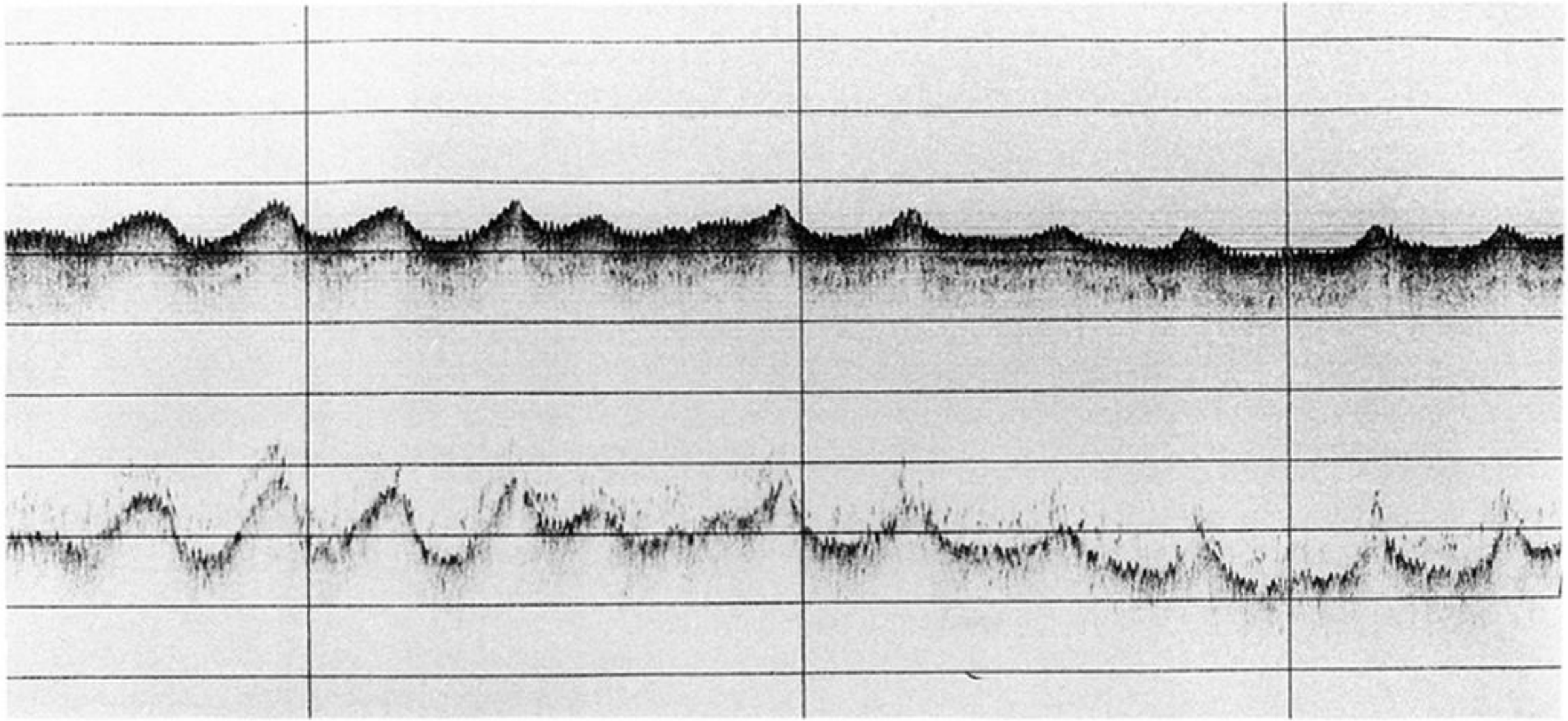

Figure 6. Part of an echo-sounding at the sand banks site, near 53° 20′ N; 2° 00′ E. The horizontal length of the transect is 8704 m, and the vertical spacing of the grid lines is 7.5 m. The asymmetric shapes of the sand waves suggests convergence of sand transport towards the centre of the transect.

PHILOSOPHICAL TRANSACTIONS OF THE ROYAL SOCIETY A MATHEMATICAL, PHYSICAL & ENGINEERING SCIENCES